Araştırma Makalesi / *Research Article* **Iğdır Üniversitesi Fen Bilimleri Enstitüsü Dergisi, 10(1): 171-178, 2020**
Fizik / Physics ***Journal of the Institute of Science and Technology,* 10(1): 171-178, 2020**

DOI: 10.21597/jist.592160 **ISSN: 2146-0574, eISSN: 2536-4618**

ABO_3-tipi Perovskitlerin Süper iletken Manyetik Histerezis Davranışları

Serkan GÜLDAL[1*]

ÖZET: ABO_3-tipi perovskitlerin süperiletken manyetik histerezis özellikleri Kaneyoshi tarafından geliştirilen etkin alan teorisi ile incelendi. ABO_3'ün merkez atomu (B) kabuk atomları (A ve O) ile antiferromanyetik etkileştiğinde tip II süperiletken davranışı gösteriyor. Böylece, B atomunun manyetik histerezis eğrisi iki zorlayıcı alan noktasına sahip oluyor (düşük zorlayıcı nokta; Hc1 ve yüksek zorlayıcı nokta; Hc2). B atomu H<Hc1olduğunda Meissner durumu, Hc1<H<Hc2 olduğunda vorteks (Abrikosov-Subnikov) ve H>Hc2 olduğunda normal durumdadır. Sonuçlarımıza göre ABO_3-tipi perovskitlerin süper iletkenlik özellikleri kabuk (O) ve merkez (B) atomlarının antiferromanyetik etkileşmesinin bir sonucudur.

Anahtar Kelimeler: ABO_3-tipi perovskitler, meissner, vortex, süperiletken, etkin alan teorisi

Superconducting magnetic hysteresis behaviors in ABO_3-type Perovskites

ABSTRACT: Superconducting magnetic hysteresis properties of the ABO_3-type Perovskites are investigated by the effective field theory. It is found that the core (B) atom of the ABO_3 exhibits type II superconducting hysteresis behaviors when it interacts antiferromagnetically with the shell (A and O) atoms. Therefore, the magnetic hysteresis curve of B atoms in the ABO_3 has binary coercive field points (lower coercivity; Hc1, and upper coercivity; Hc2). B atoms have a Meissner state at H<Hc1, vortex (or Abrikosov-Subnikov) state at Hc1<H<Hc2, and normal state at H>Hc2. Our results indicate that the superconducting properties of the ABO_3-type Perovskites result from the antiferromagnetic interaction between the shell (O) and core (B) atoms.

Keywords: ABO_3-type perovskites, meissner, vortex, superconductivity, effective field theory

[1] Serkan GÜLDAL (**Orcid ID:** 0000-0002-4247-0786), Fizik Bölümü, Fen-Edebiyat Fakültesi, Adıyaman Üniversitesi, 02040 Adıyaman

*Sorumlu Yazar/Corresponding Author: Serkan GÜLDAL, e-mail: sguldal@adiyaman.edu.tr

Geliş tarihi / *Received:* 15-07-2019
Kabul tarihi / *Accepted:* 07-11-2019

INTRODUCTION

Perovskites are typically largely ionic compounds and have the general formula ABO_3, is definite ideal cubic perovskite structure, where the eight A cations are located at the cube corners, the B cation is located at the body center of the cube, and the six anions are located at the face centers (Dongxue and Liu, 2017; O. El Rhazouani et al., 2015; Kim et al., 2014; Lang et al., 2014a; Luo and Daoud, 2015; R. Mitchell, 2002; R. H. Mitchell et al., 2000; Pandu, 2014; Tolman, 2016). After discovering this kind of perovskites which have been investigated experimentally firstly after that theoretically. Experimentally, perovskites have been synthesized and characterized to find most useful applications such as solid oxide fuel cells (Ullmann et al., 2000), sensors (Moradi et al., 2018), lasers (Weber et al., 1971), solar cells (Assadi et al., 2018), and superconductors (Cava et al., 1988; Ihringer et al., 1991; Sampathkumar et al., 1994). On the other hand, contrary to experimental studies, theoretically, fewer studies were presented. Magnetic properties of perovskites were investigated by using the Monte Carlo method (O El Rhazouani et al., 2016; El Yadari et al., 2013; Labrim et al., 2015; Masrour et al., 2016; Ngantso et al., 2016; Slassi, 2017), the Density Functional Theory and Mean Field Approximation (Dang and Millis, 2013; Keskin et al., 2008; Keskin and Polat, 2009; Lamrani et al., 2013; Zhandun and Zinenko, 2016; Zhu et al., 2017), Effective Mass Model (Yu, 2016), Mean Field Approximation (Arejdal et al., 2015; Brey et al., 2006; O El Rhazouani et al., 2014), Effective Spin Model (Deviren et al., 2011; Sanyal and Majumdar, 2009; Şarlı et al., 2015), and Green Functions Techniques (Estrada et al., 2018).

In this work, we focus on the superconducting properties of the ABO_3-type Perovskites, and we investigate the origin of the superconducting properties that perovskites by using Effective Field Theory (Braga et al., 2016; Kantar, 2017; Şarlı and Keskin, 2019a, 2019b). In this study, antiferromagnetic interaction between the shell (A and O) and core (B) atoms.

Effective Field Theory (EFT), developed by Kaneyoshi (Kaneyoshi, 1993), is a successful method to obtain the superconducting properties (type II) of the magnetic systems (Şarlı and Keskin, 2019a). Such as, superconductor core effect of the body-centered orthorhombic nanolattice structure (Şarlı, 2015), Surface superconductivity in $Ni_{50}Mn_{36}Sn_{14}$ Heusler Alloy (Duran, 2018), superconducting phase diagram of the yttrium, barium, and YBa core in $YBa_2Cu_3O_{7-\delta}$ (Keskin and Şarlı, 2018), effects of the copper and oxygen atoms of the CuO-plane on magnetic properties of the YBCO (Şarlı and Keskin, 2019b), coexistence of ferromagnetism and superconductivity in NiBi binary alloy (Şarlı and Keskin, 2019a), superconductivity-like phenomena in antiferrimagnetic endohedral fullerene with diluted magnetic surface (Padilha et al., 2013) and thermodynamic properties of copper-oxide superconductors (Kantar, 2017). In these studies, the superconducting properties (Meissner, vortex (or Subnikov and Abrikosov) and normal states) and superconducting magnetic hysteresis properties are successfully obtained by using EFT. However, superconductivity properties of Perovskites crystal system have not been investigated. Therefore, in this work, the superconductivity properties of the ABO_3-type Perovskites are investigated by using EFT.

MATERIAL AND METHOD

Since ABO_3 type perovskite is modeled and its EFT formulations are obtained as shown in **Figure 1** (Dongxue and Liu, 2017; Lang et al., 2014b; Luo and Daoud, 2015; Pandu, 2014), we shall follow the same procedures as given by as follows. In this paper, we focus on the effects of the antiferromagnetic interactions between the shell (A and O) and core (B) atoms on the magnetic properties of the ABO_3 type perovskite and its components (A, B, and O). For this aim, the temperature and external magnetic

field dependence of the magnetizations of that system are calculated for $j_{AA}>0$, $j_{AO}>0$, $j_{AB}<0$, $j_{OO}>0$, $j_{OB}>0$ (shell (A)/core (B) antiferromagnetism) and $j_{AA}>0$, $j_{AO}>0$, $j_{AB}>0$, $j_{OO}>0$, $j_{OB}<0$ (shell (O)/core (B) antiferromagnetism).

.

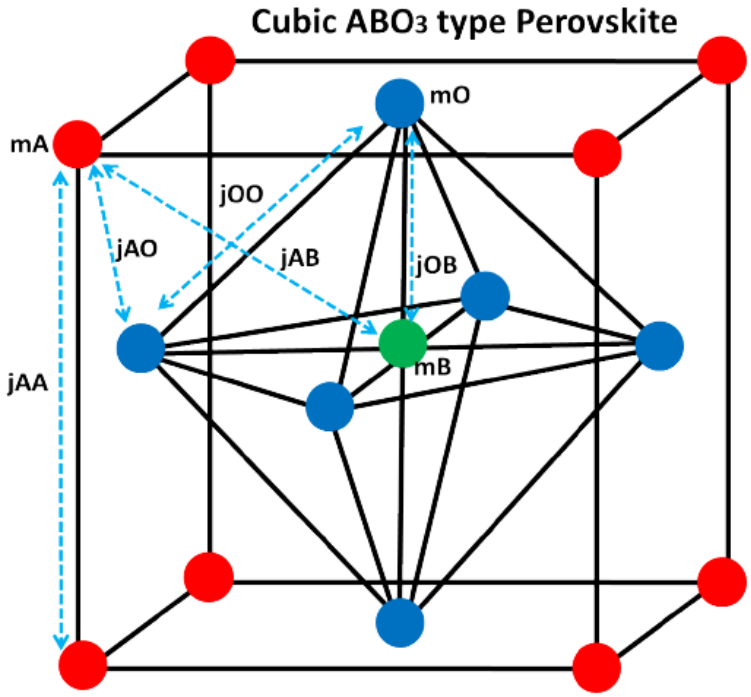

Figure 1: (Color online) ABO_3 type perovskite lattice

The Hamiltonian and magnetizations of the ABO_3 type perovskite are given by as follows:

Hamiltonian;

$$H_A = -j_{AA}\sum_{\langle A,A\rangle} S_A^z S_A^z - j_{AO}\sum_{\langle A,O\rangle} S_A^z S_O^z - j_{AB}\sum_{\langle A,B\rangle} S_A^z S_B^z - j_{OO}\sum_{\langle O,O\rangle} S_O^z S_O^z - j_{OB}\sum_{\langle O,B\rangle} S_O^z S_B^z - h\left(\sum_A S_A^z + \sum_B S_B^z + \sum_O S_O^z\right) \quad (1)$$

Magnetizations;

$$m_A = [\cosh(j_{AA}\nabla)+m_A\sinh(j_{AA}\nabla)]^3[\cosh(j_{AO}\nabla)+m_O\sinh(j_{AO}\nabla)]^3 [\cosh(j_{AB}\nabla)+m_B\sinh(j_{AB}\nabla)]^1 F_{s\text{-}1/2}(x)\big|_{x=0},$$

$$m_B = [\cosh(j_{AB}\nabla)+m_A\sinh(j_{AB}\nabla)]^8 [\cosh(j_{OB}\nabla)+m_O\sinh(j_{OB}\nabla)]^6 F_{s\text{-}1/2}(x)\big|_{x=0} \quad (2)$$

$$m_O = [\cosh(j_{OO}\nabla)+m_O\sinh(j_{OO}\nabla)]^4[\cosh(j_{OA}\nabla)+m_A\sinh(j_{OA}\nabla)]^4 [\cosh(j_{OB}\nabla)+m_B\sinh(j_{OB}\nabla)]^1 F_{s\text{-}1/2}(x)\big|_{x=0},$$

In Equations 1. and 2, $\nabla = \frac{\partial}{\partial x}$ is the differential operator and the function of $F_{1/2}(x)$ is defined in the EFT within the Ising model for the spin-1/2 Ising particles as

$$F_{1/2}(x) = \frac{1}{2}\tanh\left[\frac{1}{2}\beta(x+h)\right] \quad (3)$$

In Equation 3., $\beta=1/k_BT_A$, k_B is the Boltzmann's constant, T_A denotes the absolute temperature. We used the reduced temperature ($T=k_BT_A/J$) and reduced applied field ($H=h/J$) in all calculations. The total magnetization of ABO_3 type perovskite is given by as follows,

$$MT_{ABO_3} = \frac{1}{15}(8\, m_A + m_B + 6\, m_O) \quad (4)$$

RESULTS AND DISCUSSION

In **Figure 2**.a), the temperature dependence of the magnetizations of the A, B, O, and total ABO3 are obtained for the antiferromagnetic interaction between shell (A) and core (B) atoms ($j_{AA}>0$, $j_{AO}>0$, $j_{AB}<0$, $j_{OO}>0$, $j_{OB}>0$). The Curie temperature is at Tc=1.83. The values of the magnetizations are mA=mB=mC=$MABO_3$=0.5 at T=0 and they become zero at T=Tc. Antiferromagnetic interaction ($j_{AB}<0$) between A-B atoms causes a decreasing in the magnetization curves of the A, B, and total ABO_3 according to that of O. The most decreasing occur in the B atom (the red line). On the other hand, in **Figure 2**b), for the antiferromagnetic interaction between shell (O) and core (B) atoms ($j_{AA}>0$, $j_{AO}>0$, $j_{AB}>0$, $j_{OO}>0$, $j_{OB}<0$), magnetization curve of the B is entirely in the negative values. The values of the magnetization of the total ABO_3 is obtained as M_{ABO3}=0.43333 at T=0. One notes that the antiferromagnetism between O-B atoms has higher effects than that of the A-B atoms on the magnetizations of the ABO_3 and its components, especially in B atoms and total ABO_3.

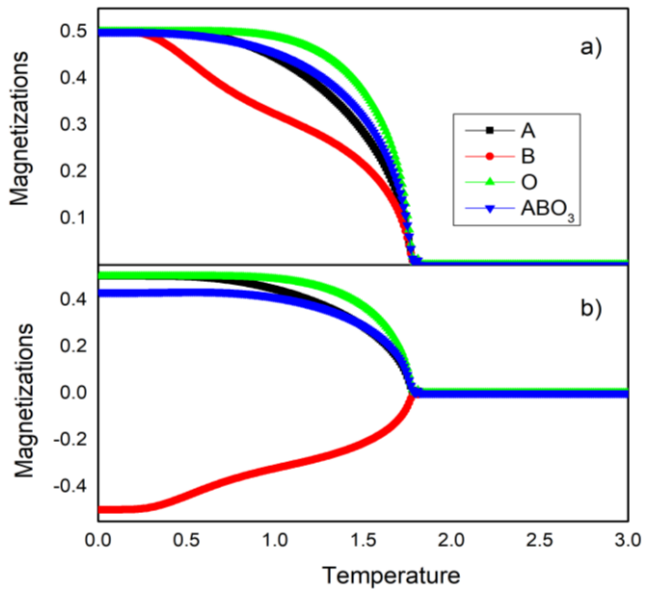

Figure 2. (Color online) Magnetizations versus temperature in ABO_3 type perovskite lattice

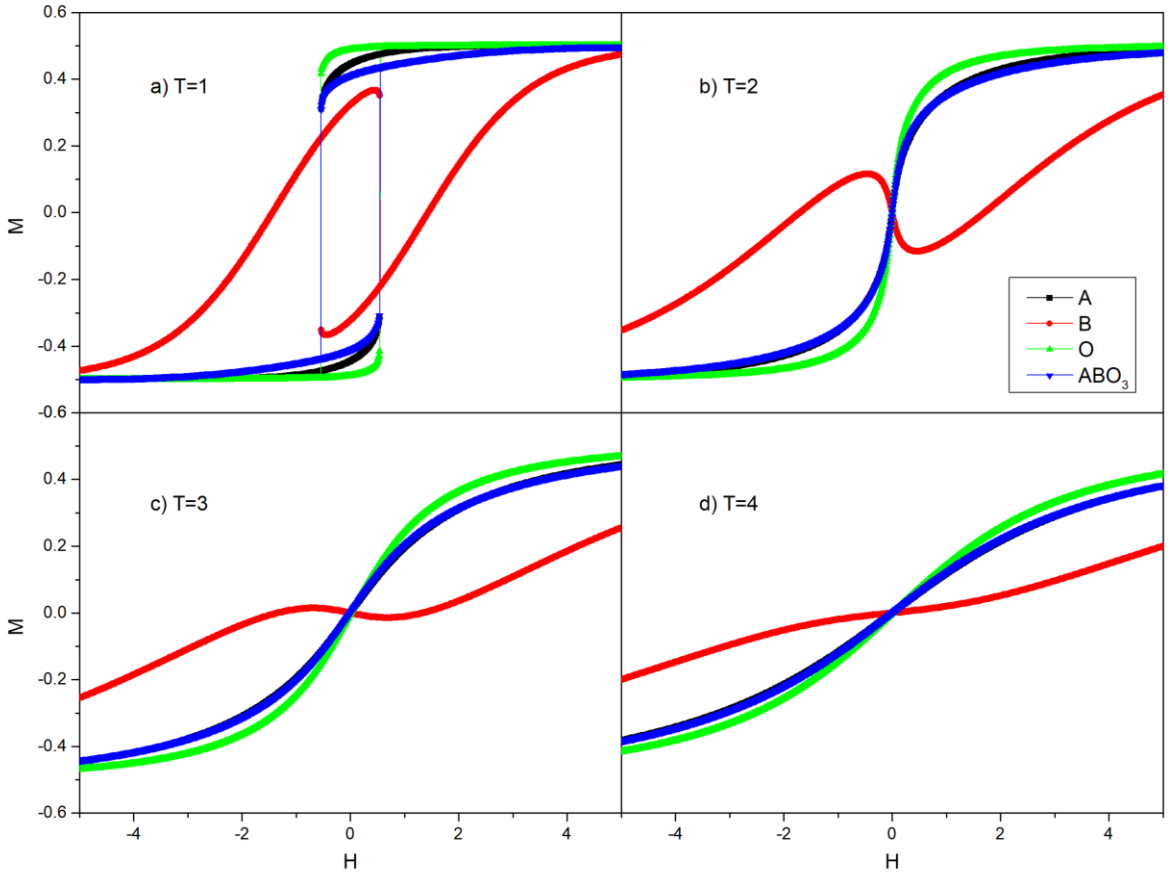

Figure 3. (Color online) Magnetizations versus external magnetic field in ABO_3 type perovskite lattice with ($j_{AA}>0$, $j_{AO}>0$, $j_{AB}>0$, $j_{OO}>0$, $j_{OB}<0$) at T=1, 2, 3, and 4 respectively

In **Figure 3**.a), .b), .c), and .d) the external field dependence of the magnetizations of the A, B, O and total ABO_3 are obtained for the antiferromagnetic interaction between shell (O) and core (B) atoms ($j_{AA}>0$, $j_{AO}>0$, $j_{AB}>0$, $j_{OO}>0$, $j_{OB}<0$) at T=1, 2, 3, and 4 respectively. The magnetic hysteresis curve of the B atom has two different coercive field point (binary coercivity) and it exhibits type II superconductivity behaviors whereas those of the A, O and total ABO_3 has one coercive field point (single coercivity) and they exhibit usual ferromagnetic hysteresis behaviors. Therefore, only M-H curves of the B atom has Meissner state at H<Hc1, vortex (or Subnikov and Abrikosov) state at Hc1<H<Hc2 and normal state at H>Hc2. Meissner state decays at Tc=1.83 and vortex (or Subnikov and Abrikosov) state decays at Tv=4. One notes that usual ferromagnetic hysteresis loop areas of the A, O and total ABO_3 disappear at Tc and type II superconducting magnetic hysteresis loop area of the B atoms disappears at Tv. Our type II superconducting magnetic hysteresis results of ABO_3 are in agreement with the theoretical results of the body-centered orthorhombic nanolattice structure (Şarlı, 2015), $Ni_{50}Mn_{36}Sn_{14}$ Heusler Alloy (Duran, 2018), yttrium, barium, copper1 and oxygen2, and YBa core of $YBa2Cu_3O_{7-\delta}$ (Keskin and Şarlı, 2018; Şarlı and Keskin, 2019b) and coexistence of ferromagnetism and superconductivity in NiBi alloy (Şarlı and Keskin, 2019a), Superconductivity-like phenomena in antiferrimagnetic endohedral fullerene (Kantar, 2017).

CONCLUSION

Superconducting magnetic hysteresis properties (type II) of the ABO_3-type Perovskites are investigated by means of the effective field theory developed by Kaneyoshi. It is found that

i. The A, O and total ABO_3 have usual ferromagnetic hysteresis behaviors and they have one coercive field point (single coercivity).
ii. The B atom of the ABO_3 has usual type II superconducting magnetic hysteresis behaviors, and it has two different coercive field point (binary coercivity).
iii. We suggest that the superconducting properties of the ABO_3-type Perovskites result from the antiferromagnetic interaction between the shell (O) and core (B) atoms

ACKNOWLEDGMENTS

This work was supported by Grant No FEFMAP/2018-0003 from Adiyaman University of Research Project Coordination (ADYUBAP), Turkey.

REFERENCES

Arejdal M, Bahmad L, Abbassi A, Benyoussef A, 2015. Magnetic properties of the double perovskite Ba2NiUO6. Physica A: Statistical Mechanics its Applications, 437 375-381.

Assadi MK, Bakhoda S, Saidur R, Hanaei H, 2018. Recent progress in perovskite solar cells. Renewable Sustainable Energy Reviews, 81 2812-2822.

Braga PR, Granado DR, Guimaraes MS, Wotzasek C, 2016. Effective field theories for superconducting systems with multiple Fermi surfaces. Annals of Physics, 374 1-15. doi:https://doi.org/10.1016/j.aop.2016.08.005

Brey L, Calderón M, Sarma SD, Guinea F, 2006. Mean-field theory for double perovskites: Coupling between itinerant electron spins and localized spins. Physical Review B, 74 (9): 094429.

Cava RJ, Batlogg B, Krajewski J, Farrow R, Rupp Jr L, White A, Short K, Peck W, Kometani T, 1988. Superconductivity near 30 K without copper: the Ba0. 6K0. 4BiO3 perovskite. Nature, 332 (6167): 814.

Dang HT, Millis AJ, 2013. Theory of ferromagnetism in vanadium-oxide based perovskites. Physical Review B, 87 (15): 155127.

Deviren B, Polat Y, Keskin M, 2011. Phase diagrams in mixed spin-3/2 and spin-2 Ising system with two alternative layers within the effective-field theory. Chinese Physics B, 20 060507. doi:10.1088/1674-1056/20/6/060507

Dongxue L, Liu Y, 2017. Recent progress of dopant-free organic hole-transporting materials in perovskite solar cells. Journal of Semiconductors, 38 (1): 011005. doi:10.1088/1674-4926/38/1/011005

Duran A, 2018. Surface Superconductivity in Ni50Mn36Sn14 Heusler Alloy. Journal of Superconductivity Novel Magnetism, 31 (12): 4053-4062. doi:10.1007/s10948-018-4686-8

El Rhazouani O, Benyoussef A, Kenz AE, 2015. Phase diagram of the double perovskite Sr2CrReO6: Effective-field theory. Journal of Magnetism and Magnetic Materials, 377 319-324. doi:10.1016/j.jmmm.2014.10.127

El Rhazouani O, Benyoussef A, Naji S, El Kenz A, 2014. Magnetic properties of double perovskite Sr2CrReO6: Mean field approximation and Monte Carlo simulation. Physica A: Statistical Mechanics its Applications, 397 31-39.

El Rhazouani O, Zarhri Z, Benyoussef A, El Kenz A, 2016. Magnetic properties of the fully spin-polarized Sr2CrOsO6 double perovskite: A Monte Carlo simulation. Physics Letters A, 380 (13): 1241-1246.

El Yadari M, Bahmad L, El Kenz A, Benyoussef A, 2013. Monte Carlo study of the double perovskite nano Sr2VMoO6. Journal of Alloys Compounds, 579 86-91.

Estrada F, Guzmán E, Navarro O, Avignon M, 2018. Curie temperature behavior in half-metallic ferromagnetic double perovskites within the electronic correlation picture. Physical Review B, 97 (19): 195155.

Ihringer J, Maichle J, Prandl W, Hewat A, Wroblewski T, 1991. Crystal structure of the ceramic superconductor BaPb 0.75 Bi 0.25 O 3. Zeitschrift für Physik B Condensed Matter, 82 (2): 171-176.

Kaneyoshi T, 1993. Differential operator technique in the Ising spin systems. Acta Physica Polonica Series A, 83 703-703.

Kantar E, 2017. Superconductivity-like phenomena in an ferrimagnetic endohedral fullerene with diluted magnetic surface. Solid State Communications, 263 31-37. doi:https://doi.org/10.1016/j.ssc.2017.07.006

Keskin M, Canko O, Polat Y, 2008. Dynamic Phase Transitions in the Kinetic Mixed Spin-1/2 and Spin-1 Ising Ferrimagnetic System under a Time-Dependent Magnetic Field. Journal of Korean Physical Society, 53 497. doi:10.3938/jkps.53.497

Keskin M, Polat Y, 2009. Phase diagrams of a nonequilibrium mixed spin-3/2 and spin-2 Ising system in an oscillating magnetic field. Journal of Magnetism and Magnetic Materials, 321 3905-3912. doi:10.1016/j.jmmm.2009.07.052

Keskin M, Şarlı N, 2018. Superconducting Phase Diagram of the Yttrium, Barium, and YBa-core in YBa2Cu3O7–δ by an Ising Model. Journal of Experimental Theoretical Physics, 127 (3): 516-524. doi:10.1134/s1063776118090157

Kim HS, Im SH, Park NG, 2014. Organolead Halide Perovskite: New Horizons in Solar Cell Research. The Journal of Physical Chemistry C, 118 (11): 5615-5625. doi:10.1021/jp409025w

Labrim H, Jabar A, Belhaj A, Ziti S, Bahmad L, Laânab L, Benyoussef A, 2015. Magnetic proprieties of La2FeCoO6 double perovskite: Monte Carlo study. Journal of Alloys Compounds, 641 37-42.

Lamrani AF, Ouchri M, Benyoussef A, Belaiche M, Loulidi M, 2013. Half-metallic antiferromagnetic behavior of double perovskite Sr2OsMoO6: First principle calculations. Journal of Magnetism Magnetic Materials, 345 195-200.

Lang L, Yang JH, Liu HR, Xiang H, Gong X, 2014a. First-principles study on the electronic and optical properties of cubic ABX3 halide perovskites. Physics Letters A, 378 (3): 290-293.

Lang L, Yang JH, Liu HR, Xiang HJ, Gong XG, 2014b. First-principles study on the electronic and optical properties of cubic ABX3 halide perovskites. Physics Letters A, 378 (3): 290-293. doi:10.1016/j.physleta.2013.11.018

Luo S, Daoud WA, 2015. Recent progress in organic–inorganic halide perovskite solar cells: mechanisms and material design. Journal of Materials Chemistry A, 3 (17): 8992-9010. doi:10.1039/c4ta04953e

Masrour R, Jabar A, Benyoussef A, Hamedoun M, Hlil E, 2016. Monte Carlo simulation study of magnetocaloric effect in NdMnO3 perovskite. Journal of Magnetism Magnetic Materials, 401 91-95.

Mitchell R. (2002). Perovskites: Modern and Ancient Almaz Press Inc. In: Ontario, Canada.

Mitchell RH, Chakhmouradian AR, Woodward PM, 2000. Crystal chemistry of perovskite-type compounds in the tausonite-loparite series,(Sr 1− 2 x Na x La x) TiO 3. Physics Chemistry of Minerals, 27 (8): 583-589.

Moradi Z, Fallah H, Hajimahmoodzadeh M, 2018. Nanocomposite perovskite based optical sensor with broadband absorption spectrum. Sensors Actuators A: Physical, 280 47-51.

Ngantso GD, Benyoussef A, El Kenz A, 2016. Monte Carlo study of magnetic properties and critical behavior of Sr2CrMoO6. Current Applied Physics, 16 (2): 211-219.

Padilha IT, de Sousa JR, Neto MA, Salmon OR, Viana J, 2013. Thermodynamics properties of copper-oxide superconductors described by an Ising frustrated model. Physica A: Statistical Mechanics its Applications, 392 (20): 4897-4904.

Pandu R, 2014. CrFe2O4–BiFeO3 Perovskite Multiferroic Nanocomposites–A Review. Material Science Research India, 11 (2): 128-145.

Sampathkumar T, Srinivasan S, Nagarajan T, Balachandran U, 1994. Properties of YBa2Cu3O7− δ-BaBiO3 composite superconductors. Applied Superconductivity, 2 (1): 29-34.

Sanyal P, Majumdar P, 2009. Magnetic model for the ordered double perovskites. Physical Review B, 80 (5): 054411.

Slassi A, 2017. Low field magnetocaloric effect in the double perovskite Sr2CrMoO6: Monte Carlo simulation. Computational Condensed Matter, 11 55-59.

Şarlı N, 2015. Superconductor core effect of the body centered orthorhombic nanolattice structure. Journal of Superconductivity Novel Magnetism, 28 (8): 2355-2363.

Şarlı N, Akbudak S, Polat Y, Ellialtioglu R, 2015. Effective distance of a ferromagnetic trilayer Ising nanostructure with an ABA stacking sequence. Physica A: Statistical Mechanics and its Applications, 434. doi:10.1016/j.physa.2015.04.002

Şarlı N, Keskin M, 2019a. Coexistence of ferromagnetism and superconductivity in NiBi-binary alloy. Chinese Journal of Physics, 60 502-509. doi:https://doi.org/10.1016/j.cjph.2019.05.029

Şarlı N, Keskin M, 2019b. Effects of the Copper and Oxygen atoms of the CuO-plane on magnetic properties of the YBCO by using the effective-field theory. Chinese Journal of Physics, 59 256-264. doi:https://doi.org/10.1016/j.cjph.2019.03.007

Tolman KR, 2016. Empirical Models for Structural Effects of A-Site Point Defects and Ordering in Perovskites.

Ullmann H, Trofimenko N, Tietz F, Stöver D, Ahmad-Khanlou A, 2000. Correlation between thermal expansion and oxide ion transport in mixed conducting perovskite-type oxides for SOFC cathodes. Solid state ionics, 138 (1-2): 79-90.

Weber M, Bass M, DeMars G, 1971. Laser action and spectroscopic properties of Er3+ in YAlO3. Journal of Applied Physics, 42 (1): 301-305.

Yu Z, 2016. Effective-mass model and magneto-optical properties in hybrid perovskites. Scientific Reports, 6 28576.

Zhandun V, Zinenko V, 2016. The effect of structural ordering on the magnetic, electronic, and optical properties of the LaPbMnSbO6 double perovskite. Journal of Alloys Compounds, 671 184-191.

Zhu XH, Xiao XB, Chen XR, Liu BG, 2017. Electronic structure, magnetism and optical properties of orthorhombic GdFeO 3 from first principles. RSC Advances, 7 (7): 4054-4061.